

## Simulating the special features of fundamental diagrams observed by Mori-Tsukaguchi and Helbing *et al*/ in uni-directional pedestrian flow

This content has been downloaded from IOPscience. Please scroll down to see the full text.

J. Stat. Mech. (2017) 023405

(<http://iopscience.iop.org/1742-5468/2017/2/023405>)

View [the table of contents for this issue](#), or go to the [journal homepage](#) for more

Download details:

IP Address: 134.148.10.12

This content was downloaded on 16/02/2017 at 20:40

Please note that [terms and conditions apply](#).

You may also be interested in:

[An experimental study on four-directional intersecting pedestrian flows](#)

Liping Lian, Xu Mai, Weiguo Song *et al*.

[Study on bi-directional pedestrian movement using ant algorithms](#)

Sibel Gokce and Ozhan Kayacan

[The physics of traffic jams](#)

Takashi Nagatani

[Fatigue effect on phase transition of pedestrian movement: experiment and simulation study](#)

Lin Luo, Zhijian Fu, Xiaodong Zhou *et al*.

[New insights into the crowd characteristics in Mina](#)

J Y Wang, W G Weng and X L Zhang

[Analysis of Phase Transition in Traffic Flow based on a New Model of Driving Decision](#)

Peng Yu, Shang Hua-Yan and Lu Hua-Pu

PAPER: Interdisciplinary statistical mechanics

# Simulating the special features of fundamental diagrams observed by Mori-Tsukaguchi and Helbing *et al* in uni-directional pedestrian flow

Cheng-Jie Jin<sup>1,2,4</sup> and Rui Jiang<sup>3</sup>

<sup>1</sup> Jiangsu Key Laboratory of Urban ITS, Southeast University of China, Nanjing, Jiangsu 210096, People's Republic of China

<sup>2</sup> Jiangsu Province Collaborative Innovation Center of Modern Urban Traffic Technologies, Nanjing, Jiangsu 210096, People's Republic of China

<sup>3</sup> MOE Key Laboratory for Urban Transportation Complex Systems Theory and Technology, Beijing Jiaotong University, Beijing 100044, People's Republic of China

E-mail: [yitaikongtiao@gmail.com](mailto:yitaikongtiao@gmail.com)

Received 29 October 2016, revised 15 December 2016

Accepted for publication 30 December 2016

Published 13 February 2017

Online at [stacks.iop.org/JSTAT/2017/023405](http://stacks.iop.org/JSTAT/2017/023405)

[doi:10.1088/1742-5468/aa5755](https://doi.org/10.1088/1742-5468/aa5755)



CrossMark

**Abstract.** The pedestrian flow dynamics are very complex. Even the fundamental diagrams of uni-directional pedestrian flow exhibit diversity. In the empirical data of Mori-Tsukaguchi and Helbing *et al*, the flows drop drastically with medium densities and nearly keep constant with high densities, which is different from many other empirical and experimental results. To simulate these special phenomena with cellular automaton (CA) models, we use the new configuration, in which the occupied area of each pedestrian is 0.4 m \* 0.2 m. The modeling framework is based on the ITP model, which is a two-process CA model presented in our previous paper, and one new rule is added: when the local density behind is below a threshold, pedestrians prefer to keep a certain front gap. With the simple rule, the new fundamental diagrams can qualitatively coincide with the empirical facts of Mori-Tsukaguchi and Helbing *et al*. Some other results, including simulation patterns and velocities of pedestrians can further confirm the validity of the new rule, and give some explanations for the diversity of different empirical data. These results are useful contributions for pedestrian flow modeling.

**Keywords:** traffic and crowd dynamics, traffic models, nonlinear dynamics

<sup>4</sup> Author to whom any correspondence should be addressed.

---

## Contents

1. <b>Introduction</b>	2
2. <b>The rules of the basic model</b>	4
3. <b>The new rule considering the reserved front gap and the local density behind</b>	5
4. <b>Simulation results</b>	7
5. <b>Conclusion</b>	12
<b>Acknowledgments</b>	13
<b>References</b>	13

---

## 1. Introduction

The study of pedestrian flow is an important task, which has a long history [1]. Many different approaches can be used in the simulation of pedestrian flow, including the macroscopic ones in which the flow-density and velocity-density relationship is discussed, and the microscopic ones in which the movement of each pedestrian is presented. The latter can be further classified into several types, and in this paper we concentrate on one simple but useful type: cellular automaton (CA) model.

In CA models the time and space are both discretized, which makes the computer simulation fast and easy to run [2]. They can be used for many different situations in the field of pedestrian flow simulations, including the counterflow in a corridor [3, 4], the intersecting flows [5], evacuation process in a room [6, 7], etc. But during these years, there are not so many studies concerning the over-crowded uni-directional flow. Although it seems simple, the complexity and diversity cannot be simply ignored, and until now, some problems are still not solved.

One of the problems is the situation with high densities (larger than  $6 \text{ m}^{-2}$ ). In most previous studies using CA models, the occupied area of each pedestrian is set as  $0.4 \text{ m} \times 0.4 \text{ m}$ , which means the maximum density is only  $6.25 \text{ m}^{-2}$ . In many previous experiments of pedestrian flow [8–13], this density cannot be reached, and the maximum value is just between  $4\text{--}6 \text{ m}^{-2}$ . However, some pedestrian flow situations with high densities exist in real life. For example, as shown in figure 1, in the data of Hankin-Wright [14] the jam density is also between  $4\text{--}6 \text{ m}^{-2}$ . But in the empirical data of Mori-Tsukaguchi [15] and Helbing *et al* [16], we can find many data points with high densities, which are between  $6\text{--}10 \text{ m}^{-2}$ . Especially in the data of Helbing *et al* [16], we can see that with medium densities (about  $5\text{--}6 \text{ m}^{-2}$ ), the flows drop drastically. But

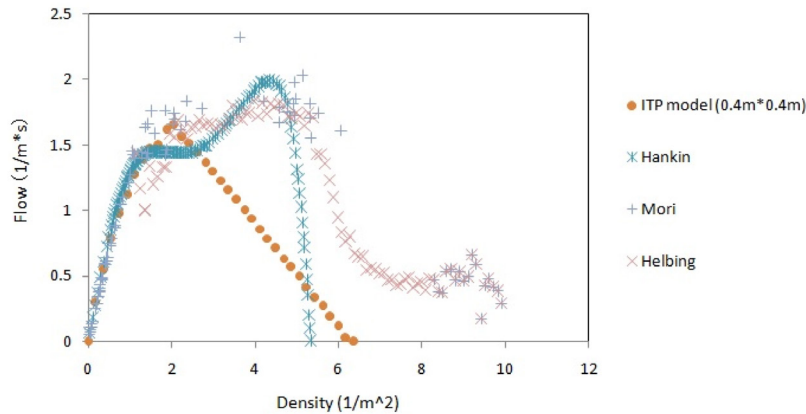


**Figure 1.** The empirical and simulated fundamental diagrams of uni-directional flows. The three empirical datasets [14–16] are obtained from the work of Zhang *et al* [10], which can be downloaded at [www.asim.uni-wuppertal.de/en/database-new/data-from-literature.html](http://www.asim.uni-wuppertal.de/en/database-new/data-from-literature.html). The simulation results are that of ITP model [21]. It is a traditional CA model in which each pedestrian occupies the area of  $0.4 \text{ m} * 0.4 \text{ m}$ .

with high densities, the flows nearly keep constant (and even increase a little). This irregular curve is quite different from the simulation results in many previous papers, which usually have the regular shape of a triangle or a parabolic curve [12, 13, 17–21], no matter they are simulated by CA models or not. One typical example of these traditional results is that of the ITP model [21], which is also shown in figure 1 for comparisons. It is clear that this type of models cannot well reproduce the uni-directional flow under high-density condition.

In recent years, some researchers try to use some special ideas to simulate the pedestrian flow under high-density condition. For example, Bandini *et al* [22] allow transient pedestrians overlapping in high density situations; Feliciani and Nishinari [23] introduce additional nodes located in the middle of adjacent cells, etc. In these studies with CA models, the model rules are complex, but the shapes of fundamental diagrams do not essentially change, and the properties reported in the data of Helbing *et al* [16] still cannot be simulated.

Therefore, we think something new is needed. Since under high-density condition pedestrians usually occupy smaller area, we set it as  $0.4 \text{ m} * 0.2 \text{ m}$ . This configuration can significantly enhance the flows and velocities of uni-directional flow. Then we introduce one new rule, which make pedestrians keep certain front gap when the local density behind is below a threshold. The new rules can change the shape of the fundamental diagrams, and reproduce some important phenomena in the data of Helbing *et al* [16], e.g. the flow drops quickly with medium densities and nearly keeps constant with high densities. It is a useful contribution to the modeling of pedestrian flow.

This paper is organized as follows. The rules of the previous ITP model are briefly presented in section 2. The new rule which considers the reserved front gap and the local density behind, are discussed in section 3. The simulation results are presented in section 4. The conclusion and discussions are given in section 5.

## 2. The rules of the basic model

Here we briefly recall the rules of the ITP model, which has been discussed in our previous paper [21]. It is an improved version of the ‘two-process’ model [24–26], in which the forward movement and the lateral movement of pedestrians are split and handled at two different sub-steps. In order to describe the pedestrian movements more accurately, the size of one cell is set to 0.1 m \* 0.1 m. Since the space occupied by a pedestrian is a square of 0.4 m \* 0.4 m, in the model each pedestrian occupies  $4 * 4 = 16$  cells. The time step is set to 1 s.

The schematic illustration of the pedestrian moving is shown in figure 2. The parameters used in the ITP model are defined as follows:

This model can be used for the simulation of bi-directional flow, as present in [21]. Since in this paper we only discuss the modeling of uni-directional flow, the rules will become simpler than before. Now the basic rules are:

1. Calculate the front gap and two lateral gaps of each pedestrian (see explanation 1a below).
2. Judge whether lateral movement is needed (see explanation 2a below). If the answer is yes, record the potential plan (see explanation 2b below).
3. Fulfill the parallel update of lateral movement. If there exist conflicts, the movement has to be abandoned.
4. Fulfill the forward movement (see explanation 4a below).

The further explanations of the corresponding rules are:

- 1a. If there is no pedestrian in the front/lateral direction, the gap is the distance to the corresponding boundary.
- 2a. If  $V_i > G_a$ , the lateral movement is needed.

This rule is similar to the model rule in multilane vehicular traffic flow, which means that the forward movement is hindered by the ‘key one’.

2b. Some points should be noted:

- (1) A pedestrian tries to move to right firstly; if failed, then he/she tries to move to left.
- (2) The exhaustive range of  $V_b$  is: 0.1, 0.2, ...,  $\min(G_b, V_{b\max})$ . Find the smallest velocity which can help the pedestrian become ‘better’, and record the value.
- (3) Suppose the front gaps before (after) the lateral move are  $G_{a1}$  ( $G_{a2}$ ), here ‘better’ means  $G_{a1} < G_{a2}$ , i.e. the front gap becomes larger.
- (4) If the pedestrian tries to move to left and (2) (3) are both fulfilled, there is still 50% chance to give up the lateral movement.

4a. There are three different situations to be considered:

$$(1) \quad \text{If } V_a > G_a, V_a \rightarrow \begin{cases} G_a & P_1 = 0.9 \\ \min(G_a - AD, 0) & P_0 = 0.1. \end{cases}$$

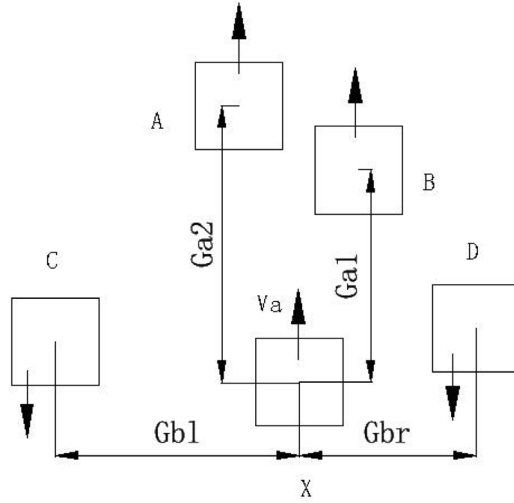


**Figure 2.** An example of the surrounding environment of a pedestrian  $X$ . We call the nearest pedestrian in the moving direction as ‘key one’, and Pedestrian  $B$  is the ‘key one’ of pedestrian  $X$ .  $G_{a1}$ ,  $G_{a2}$ ,  $G_{bl}$  and  $G_{br}$  denote distances between pedestrian  $X$  and other pedestrians in the neighborhood, see the main text.  $G_a$ : the front gap to the nearest pedestrian. In figure 1,  $G_a = G_{a1}$  since  $G_{a1} < G_{a2}$ .  $G_{bl}$  ( $G_{br}$ ): the lateral gap to the nearest pedestrian on the left (right) side.  $V_a$ : the front velocity. The maximum is  $2 \text{ m s}^{-1}$  in the ITP model.  $V_b$ : the lateral velocity. The maximum is  $1 \text{ m s}^{-1}$  in the ITP model.  $V_t$ : the pedestrian-dependent preferred front velocity, which is assumed to be uniformly distributed over the interval  $(1.0 \text{ m s}^{-1}, 2.0 \text{ m s}^{-1})$ . It implies the average velocity of pedestrians when they are moving freely is  $1.5 \text{ m s}^{-1}$ , which is close to the value in many previous empirical studies. Here only the discrete value of  $1.0, 1.1, 1.2, \dots, 1.9, 2.0$  can be chosen. AD: An acceleration/deceleration value used in the update of forward movement, which is set as  $0.1 \text{ m s}^{-2}$  in the ITP model.

The random deceleration rule is similar to that in many CA models. Here the randomization probability is set as 0.1.

$$(2) \text{ If } V_a \leq G_a \text{ and } V_a < V_t, V_a \rightarrow \begin{cases} \min(V_t, G_a) & P_1 = 0.9 \\ V_a & P_0 = 0.1 \end{cases}$$

$$(3) \text{ If } V_a \leq G_a \text{ and } V_a \geq V_t, V_a \rightarrow \begin{cases} V_a + \text{AD} & P_0 = 0.1 \\ V_a & P_2 = 0.8 \\ V_a - \text{AD} & P_0 = 0.1. \end{cases}$$

The latter two rules have also considered the random fluctuation of front velocity.

### 3. The new rule considering the reserved front gap and the local density behind

In many previous studies, there are only two typical states in the fundamental diagrams of pedestrian flow model: the free flow and the stop-and-go waves. Actually, this is the main problem of modeling uni-directional flow, since in the study of Helbing *et al*

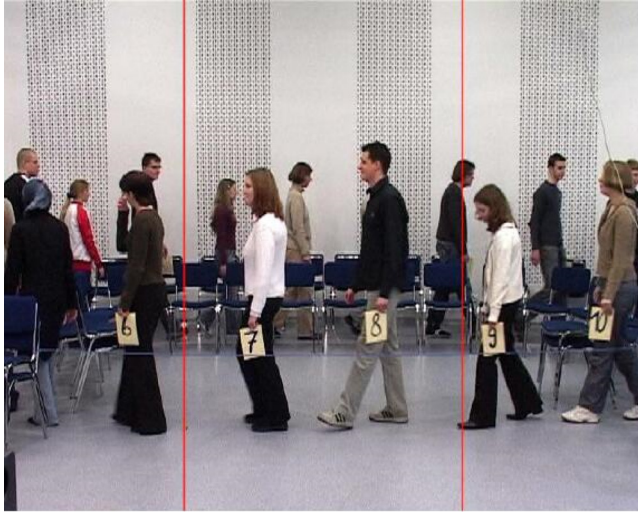


**Figure 3.** One typical snapshot in the video of a pedestrian experiment, when people are moving along a circular route, and everybody has enough room. Reproduced with permission from [8].

[16], it is reported that there are three different states: the laminar flow (the free flow), the stop-and-go waves and the irregular flows named ‘crowd turbulence’. In the crowd turbulence, it is said that ‘people are so densely packed that they were moved involuntarily by the crowd’. With the increase of density, the transition from stop-and-go waves to crowd turbulence will suddenly occur. Sometimes since the pressure are too unbearable, ‘people try to escape the crowd and start pushing to gain space’, which is called ‘crowd panic’. It is a very special state, which is quite different from the stop-and-go waves.

Therefore, we think new rules and configurations are needed to simulate the crowd turbulence and the sudden transition. The first step is about the occupied area of each pedestrian. In the ordinary configuration of pedestrian flow simulation with CA models, the occupied area of each pedestrian is  $0.4 \text{ m} * 0.4 \text{ m}$ . This configuration implies everybody has a large room, the connection between people is usually weak, and the body contacts will seldom occur. As shown in one typical snapshot (see figure 3), everybody knows there is no need to hurry and they are usually very relaxed. Then the jam density could be very low, e.g. between  $4\text{--}6 \text{ m}^{-2}$ . Even when the culture differences between different countries (e.g. Germany and India [27]) are considered and studied, the jam densities in these experiments still do not exceed  $6 \text{ m}^{-2}$ .

But when the density is very high, the situation will be different. For example, the data of Helbing *et al* [16] come from the Hajj pilgrimage, when up to 3 million Muslims perform the stoning ritual within 24h. In such a special environment, people just want to move forward as soon as possible, and do not consider the need of privacy. Then the jam density could be  $10 \text{ m}^{-2}$  or even larger.

For this situation, we can use a simple method to solve the problem in the simulation: just set the occupied area of each pedestrian as  $0.4 \text{ m} * 0.2 \text{ m}$ , and let each pedestrian occupy  $4 * 2 = 8$  cells. Here the width is  $0.4 \text{ m}$  and the length is  $0.2 \text{ m}$ . For this configuration, the jam density will be  $12.5 \text{ m}^{-2}$ . Thus it is easy to explain the empirical data points [15, 16] in which the densities are between  $6\text{--}10 \text{ m}^{-2}$ . In all the following simulations, the configuration of  $0.4 \text{ m} * 0.2 \text{ m}$  is always adopted.

The second step is about the new rule. According to the description of Helbing *et al* [16], when the pressure is larger than a critical value, the transition will occur and the movement of pedestrians will change. Thus we use a new rule to reproduce this phenomenon:

$$\text{If } G_a \leq 0.1 * K \text{ and } D_L \leq M, \quad V_a = 0.$$

It is added into the Rule 4 (fulfill the forward movement) of section 2. It means pedestrian tries to reserve some distance with the front one, when they are relaxed; but when the local density behind is larger than  $M$ , the pedestrian will be pushed from behind and move forward again.

Here  $D_L$  is the local density behind the pedestrian within the distance of  $L$ , and  $M$  is a critical value between 0 and 1.  $K$  is a critical value representing the preferred reserved gap of pedestrians. The local density is not a new idea, which has been discussed in some previous papers [20] and voronoi method is often used. Here we just consider the situation exactly behind the pedestrian, i.e. the width is 0.4 m.

We would like to mention that our new rule can mimic the isotropic feature of over-crowded pedestrian flow. Different from normal fluid such as water or air, the vehicular flow and the pedestrian flow are usually regarded as anisotropic flow, in which vehicles or pedestrians will not be influenced by the ones behind. However, for over-crowded situation, pedestrians will be pushed forward by the ones behind. Thus the pedestrian flow looks like normal fluid and exhibits isotropic feature. In our new rule, the parameters  $M$  is introduced to reflect the transition between anisotropic and isotropic features.

#### 4. Simulation results

This section presents the simulation results of the new model. We study the fundamental diagrams obtained under the periodic boundary conditions. Initially, all the pedestrians are distributed randomly on the square lattice of  $S * W$ . Firstly we set  $S = 200$  cells = 20 m = 100 pedestrians and  $W = 40$  cells = 4 m = 10 pedestrians. In the following diagrams, the velocity  $v$  is the averaged value of the front velocity (the lateral velocity is not considered). We run 3600 time steps to remove the transient state. Then the averaged velocities of all the pedestrians are recorded during another 1800 time steps. The flow  $J$  is obtained by  $J = \rho * v$ , in which  $\rho$  is the pedestrian density. The results presented in the figures are all averaged over 50 simulations.

In figure 4<sup>5</sup>, the parameters are  $(K, L, M)$ , e.g. (4, 10, 0.8) means  $K = 4$ ,  $L = 10$  cells,  $M = 0.8$ . Here (0, 0, 0) implies the model without the new rule. The flows of (0, 0, 0) are higher than the empirical values under high densities, which means only the introduction of new configuration cannot simulate these phenomena well. However, some other results qualitatively coincide with the empirical data of Helbing *et al*, especially the curve of (4, 10, 0.9): the flows drop drastically with medium densities, and keep nearly

<sup>5</sup> Since the main topic of this paper is the high-density condition, for simplicity, in the following diagrams we will not show the data of Hankin-Wright again. In order to make the figures clear, in all the following fundamental diagrams, we will not show the left part of all the simulated curves except the original model with the configuration of 0.4 m \* 0.2 m, since they always completely coincide when densities are low.

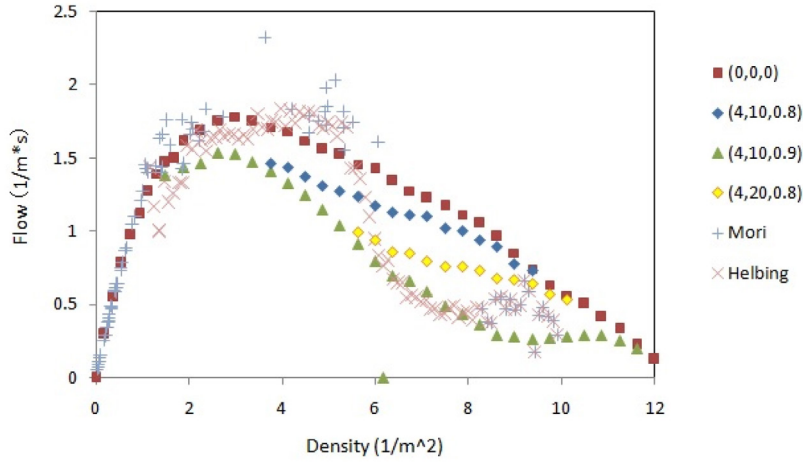


**Figure 4.** The fundamental diagrams when new rule is added. Here the parameters are  $(K, L, M)$ , e.g.  $(4, 10, 0.8)$  means  $K = 4$ ,  $L = 10$  cells,  $M = 0.8$ . Two empirical datasets are presented for comparisons.

constant with high densities. The turning point is at about  $8 \text{ m}^{-2}$ , which is close to the empirical result. The jam density is still  $12.5 \text{ m}^{-2}$ .

And then, we consider the situation when  $L = 20$  cells, and  $M$  can be set as 0.85. The curve of  $(4, 20, 0.8)$  is also shown in figure 4, which is just in the middle of  $(4, 10, 0.8)$  and  $(4, 10, 0.9)$ . We also try some other parameters, but the results are not presented here, since they are similar to others. For example, the curve of  $(4, 20, 0.85)$  is similar to that of  $(4, 10, 0.9)$ .

The effect of the new rule can be further checked by the simulation results with the same density under periodic boundary conditions. The typical simulation patterns are shown in figure 5, and the velocities of each pedestrian are presented in figure 6, while some important velocity features are shown in table 1. We do not have the empirical data of standard deviation (SD) and relative standard deviation (RSD), so we only present the empirical data of averaged velocity in the tables. It is clear that for  $(0, 0, 0)$ , the pedestrians are distributed homogeneously. The RSD is smaller, which means the fluctuation of the velocities of each pedestrian is not large. Although some of the pedestrians stop, most of them keep moving with small velocities. But for  $(4, 10, 0.9)$ , many pedestrians stand together and cannot move, while some others have large room and move forward with high velocities. The RSD is much larger. We find the two states are similar to the homogeneous state and jammed state in the initial distributions of vehicular traffic flow modeling [28]. Of course, the jammed state of  $(4, 10, 0.9)$  is closer to the stop-and-go waves observed in empirical pedestrian flow data, especially when the simulated averaged velocity is closer to the empirical value.

When the density is even higher, the new situations are presented in figures 7 and 8, and the new statistics are shown in table 2. Since there are too many pedestrians in a small region, the difference between figures 7(a) and (b) seems not obvious. But in figure 8, it is clear that for  $(0, 0, 0)$ , many pedestrians move together and the velocities are homogeneous, which is far from reality. For  $(4, 10, 0.9)$ , the structure is similar to figure 6(b), in which only some pedestrians can move and the velocities are not homogeneous. The feature exhibited in table 2 is similar to that in table 1, since the RSD of  $(4, 10, 0.9)$  is much larger than that of  $(0, 0, 0)$ . As mentioned in [16], this state is very

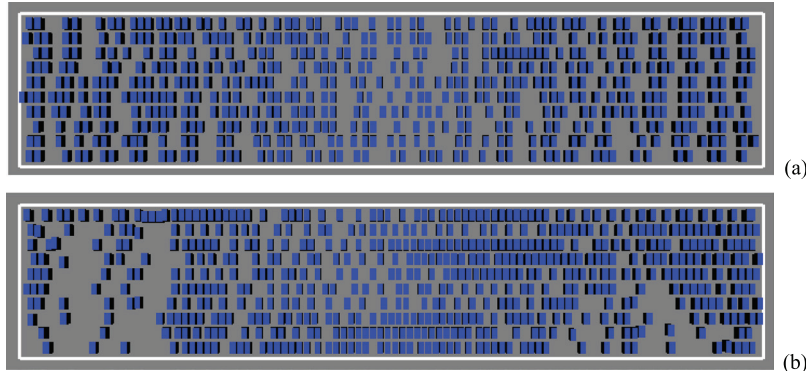


**Figure 5.** The simulation patterns of different states of uni-directional flow when  $\rho = 7.5 \text{ m}^{-2}$ . (a)  $(K, L, M) = (0, 0, 0)$ ; (b)  $(K, L, M) = (4, 10, 0.9)$ .

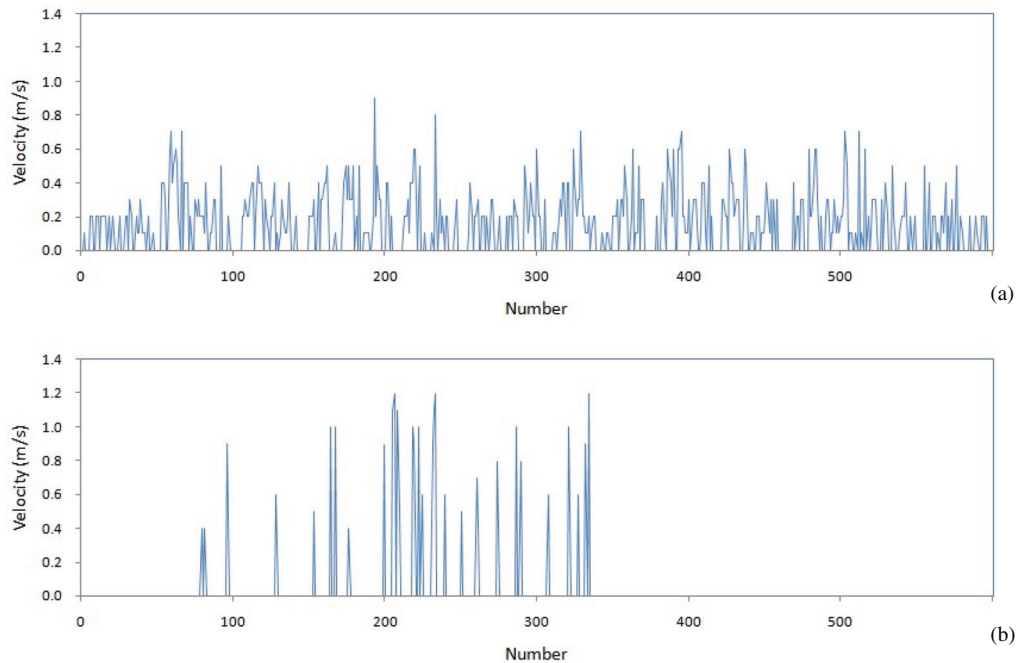


**Figure 6.** The velocities of each pedestrian in uni-directional flow when  $\rho = 7.5 \text{ m}^{-2}$ . (a)  $(K, L, M) = (0, 0, 0)$ ; (b)  $(K, L, M) = (4, 10, 0.9)$ .

**Table 1.** The comparison of velocity features at  $\rho = 7.5 \text{ m}^{-2}$ .

Parameters	Averaged velocity ( $\text{m s}^{-1}$ )	Standard deviation (SD)	Relative standard deviation (RSD)
$(K, L, M) = (0, 0, 0)$	0.156	0.179	1.15
$(K, L, M) = (4, 10, 0.9)$	0.065	0.191	2.93
Empirical data	0.058	Not available	Not available

dangerous and accidents can easily occur. The velocity differences between adjacent pedestrians can become pressures under high-density condition.

The characteristics under high-density condition also can be seen in figure 9. Here we present the proportion of pedestrians who are stopped under high densities. It is easy to understand that for  $(0, 0, 0)$ , the curve increases monotonically, which means

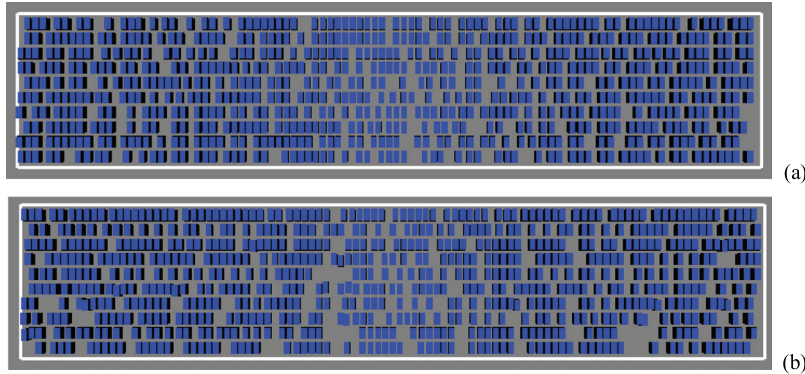


**Figure 7.** The patterns of different states of uni-directional flow when  $\rho = 9 \text{ m}^{-2}$ . (a)  $(K, L, M) = (0, 0, 0)$ ; (b)  $(K, L, M) = (4, 10, 0.9)$ .

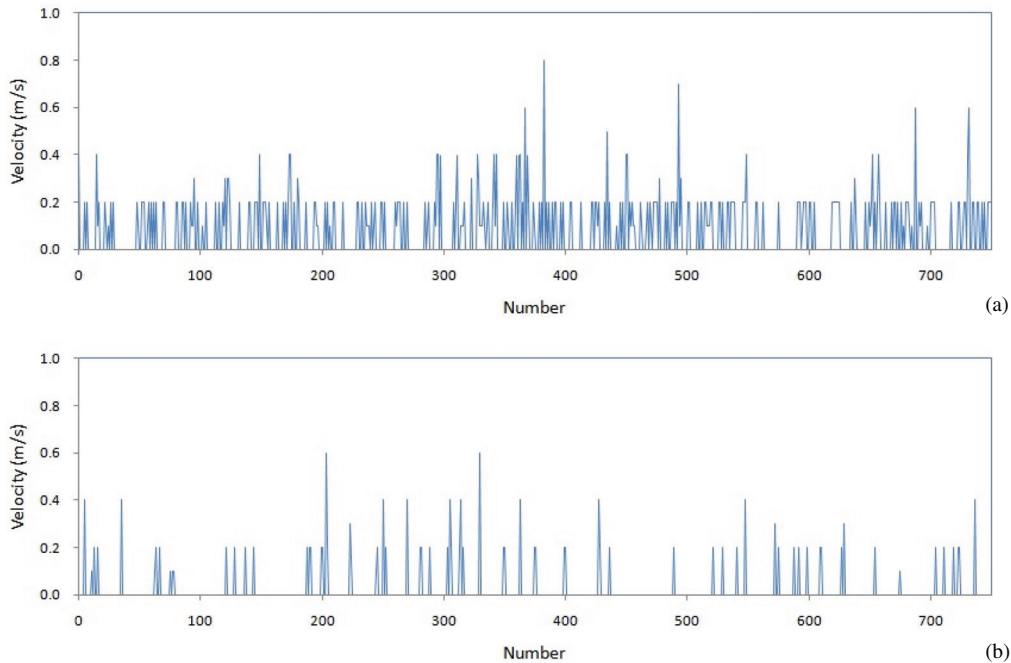


**Figure 8.** The velocities of each pedestrian in uni-directional flow when  $\rho = 9 \text{ m}^{-2}$ . (a)  $(K, L, M) = (0, 0, 0)$ ; (b)  $(K, L, M) = (4, 10, 0.9)$ .

**Table 2.** The comparison of velocity features at  $\rho = 9 \text{ m}^{-2}$ .

Parameters	Averaged velocity ( $\text{m s}^{-1}$ )	Standard deviation (SD)	Relative standard deviation (RSD)
$(K, L, M) = (0, 0, 0)$	0.095	0.118	1.24
$(K, L, M) = (4, 10, 0.9)$	0.031	0.077	2.48
Empirical data	0.052	Not available	Not available

the state of pedestrian flow does not change. But for  $(4, 10, 0.9)$ , it is clear that at  $\rho = 9 \text{ m}^{-2}$ , the proportion starts decreasing, and keeps nearly constant within a certain density range (around  $\rho = 10 \text{ m}^{-2}$ ). This change implies one complex transition: it is the effect of the new rule, which means some pedestrians start moving again due to

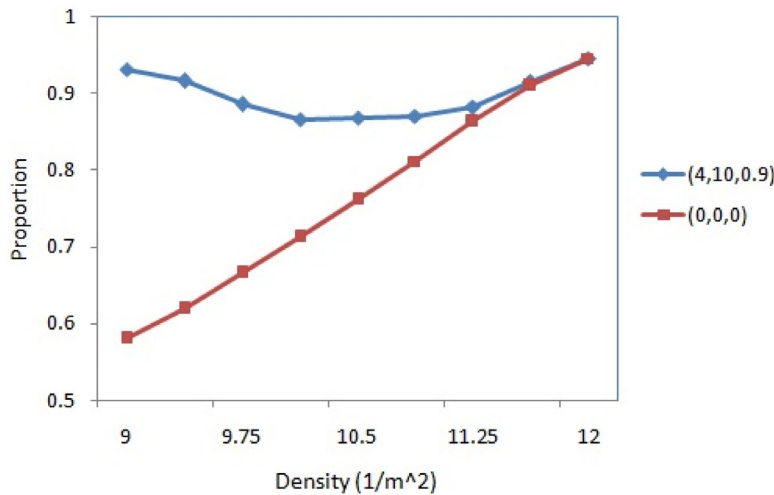


**Figure 9.** The proportion of pedestrians who are stopped under high densities.

high densities behind. It can produce the phenomena which are similar to ‘crowd turbulence’ in [16].

Note that the empirical data of fundamental diagram seems to exhibit a double-peaks structure. Our simulation results of (4, 10, 0.9) partially described the double-peaks form. As mentioned above, the emergence of the second peak might be due to the minimum proportion of stopped pedestrians.

Now we consider a special case  $L = 0$  and  $K > 0$ . In this case,  $M$  becomes meaningless, and the rule will be:

$$\text{If } G_a \leq 0.1 * K, \quad V_a = 0.$$

It means pedestrians always reserve some distance from the front one, and they always feel relaxed. Here  $K$  cannot be too large, otherwise it will be unrealistic.

The results of  $K = 0, 2, 4$  when  $L = 0$  are shown in figure 10. It can be seen that the flows decrease under high-density conditions, and the jam density also becomes smaller. The phenomenon of ‘crowd turbulence’ disappears, and the shape of the curve is similar to parabola. These results imply that when the local density (also the pressure) behind is not considered, the uni-directional flow will become slower, but also more regular and safer.

Finally we study the influence of lateral move on uni-directional flow. The number of pedestrian lane is set as  $N$ , so  $W = 0.4 \text{ m} * N$ . The simulation results of different system widths are shown in figure 11. It can be seen that the curve of  $K = 0, N = 1$  is similar to that of  $K = 0, N = 10$ , which implies in a homogeneous state of many lanes without the consideration of reserved front gap, the effect of lateral move is not obvious. But the curve of  $K = 4, N = 1$  is different from that of  $K = 4, N = 10$ , which means when the reserved front gap is considered, the lateral move can help to increase the gap and enhance both the flows and velocities under high-density condition. Finally, the most important point is that the shapes of fundamental diagrams do not change in figure 11, which means the lateral move is not the main reason for the occurrence of crowd turbulence in the data of Helbing *et al* [16]. Nevertheless, the various results in figures 10 and 11 can help to explain the large diversity of flows and jam densities in different empirical data.

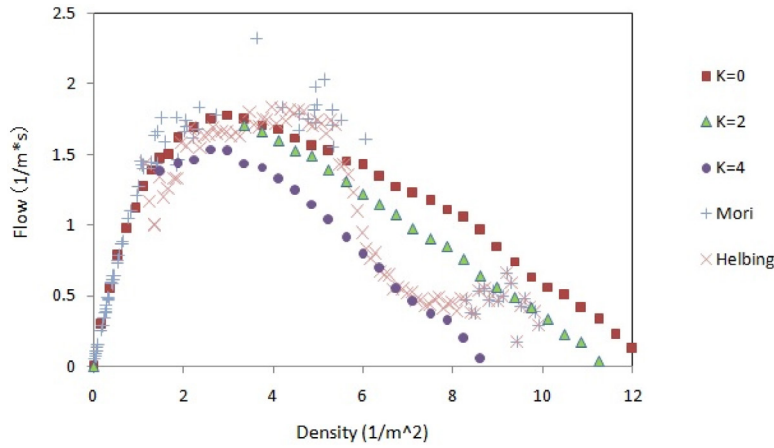


**Figure 10.** The new fundamental diagrams when  $L = 0$ . Two empirical datasets are presented for comparisons.

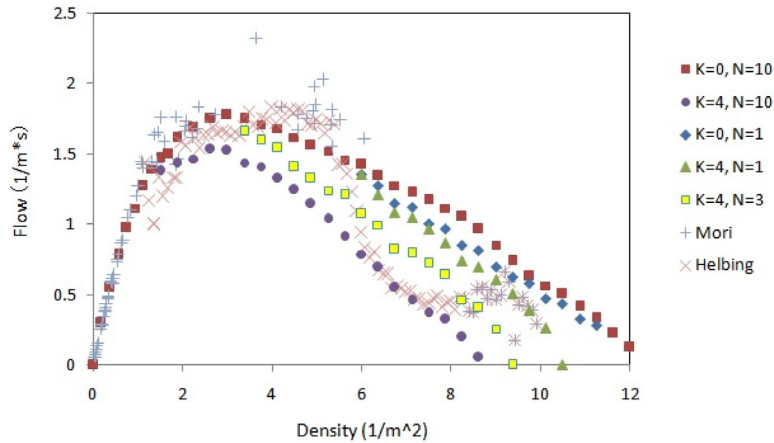


**Figure 11.** The fundamental diagrams when different system widths ( $N$ ) are considered and  $L = 0$ . Two empirical datasets are presented for comparisons.

## 5. Conclusion

In this paper we discuss the simulation of some special phenomena in uni-directional pedestrian flow, which are reported in the empirical data of Mori-Tsukaguchi and Helbing *et al.* Since the traditional configuration in which each pedestrian occupies the area of  $0.4 \text{ m} \times 0.4 \text{ m}$  cannot simulate the uni-directional flow under high-density condition, we set the new occupied area as  $0.4 \text{ m} \times 0.2 \text{ m}$ . Then we introduce one simple rule, which makes pedestrians keep certain front gap when the local density behind is below a threshold. It can produce more reasonable fundamental diagrams for the uni-directional flow. The situation reported in the data of Helbing *et al.*, in which the stop-and-go waves are found with medium densities and the crowd turbulence appear with high densities, can be realized by the new rule. The transition between them can be simulated by the change of the local density behind. And we also discuss some special situations, which can help to explain the diversity in different empirical data. We think these results can be useful contributions for the pedestrian flow modeling.

Although we have made some progress, there are still some problems to be solved. For example, even in the model of  $0.4 \text{ m} \times 0.2 \text{ m}$  without the new rule, the maximum flow is a little smaller than all the empirical values. When new rule is added, the differences under medium-density condition become larger. Besides, the critical densities are still smaller in the simulation results. Maybe it implies that in pedestrian flow, there are still some potential mechanisms which we are not aware of, e.g. the complex anticipation effects of pedestrians.

Another problem is the lack of enough empirical data. Due to the safety concern, the pedestrian experiment with high densities is not easy to organize, and the panic cannot be simulated well in a relaxed environment. Only in some special environment, people can have the willingness to occupy smaller area and endure frequent body contacts. Maybe we need to get more empirical data from the real life, especially in some large-scale events with many people on some special dates (e.g. festivals or ceremonies in China), and find more empirical fundamental diagrams to compare with the data of Mori-Tsukaguchi and Helbing *et al.* The large diversity between various empirical data of pedestrian flow still needs to be explained more systematically.

## Acknowledgments

This work was funded by the National Natural Science Foundation of China (No. 11302022, 11422221, 71371175, 71621001), and the Natural Science Foundation of Jiangsu Province (No. BK20150619).

## References

- [1] Papadimitriou E, Yannis G and Golias J 2009 A critical assessment of pedestrian behaviour models *Transp. Res. F* **12** 242–55
- [2] Wolfram S 1983 Statistical mechanics of cellular automata *Rev. Mod. Phys.* **55** 601–44
- [3] Muramatsu M, Irie T and Nagatani T 1999 Jamming transition in pedestrian counter flow *Physica A* **267** 487–98
- [4] Tajima Y, Takimoto K and Nagatani T 2002 Pattern formation and jamming transition in pedestrian counter flow *Physica A* **313** 709–23
- [5] Helbing D, Buzna L, Johansson A and Werner T 2005 Self-organized pedestrian crowd dynamics: experiments, simulations, and design solutions *Transp. Sci.* **39** 1–24
- [6] Burstedde C, Klauck K, Schadschneider A and Zittartz J 2001 Simulation of pedestrian dynamics using a two-dimensional cellular automaton *Physica A* **295** 507–25
- [7] Kirchner A and Schadschneider A 2002 Simulation of evacuation processes using a bionics-inspired cellular automaton model for pedestrian dynamics *Physica A* **312** 260–76
- [8] Seyfried A, Steffen B, Klingsch W and Boltes M 2005 The fundamental diagram of pedestrian movement revisited *J. Stat. Mech.* **P10002**
- [9] Kretz T *et al* 2006 Experimental study of pedestrian counterflow in a corridor *J. Stat. Mech.* **P10001**
- [10] Zhang J, Klingsch W, Schadschneider A and Seyfried A 2012 Ordering in bidirectional pedestrian flows and its influence on the fundamental diagram *J. Stat. Mech.* **P02002**
- [11] Seitz M J and Köster G 2012 Natural discretization of pedestrian movement in continuous space *Phys. Rev. E* **86** 046108
- [12] Guo N *et al* 2016 Uni- and bi-directional pedestrian flow in the view-limited condition: experiments and modeling *Transp. Res. C* **71** 63–85
- [13] Nikolic M, Bierlaire M, Farooq B and de Lapparent M 2016 Probabilistic speed-density relationship for pedestrian traffic *Transp. Res. B* **89** 58–81
- [14] Hankin B D and Wright R A 1958 Passenger flow in subways *Oper. Res. Q.* **9** 81

- [15] Mori M and Tsukaguchi H 1987 A new method for evaluation of level of service in pedestrian facilities *Transp. Res. A* **21** 223–34
- [16] Helbing D, Johansson A and Al-Abideen H 2007 Dynamics of crowd disasters: an empirical study *Phys. Rev. E* **75** 046109
- [17] Schadschneider A and Seyfried A 2009 Validation of CA models of pedestrian dynamics with fundamental diagrams, cybernetics and systems *Int. J.* **40** 367–89
- [18] Fu Z *et al* 2016 Effect of speed matching on fundamental diagram of pedestrian flow *Physica A* **458** 31–42
- [19] Flötteröd G and Lämmel G 2015 Bidirectional pedestrian fundamental diagram *Transp. Res. B* **71** 194–212
- [20] Xiao Y, Gao Z, Qu Y and Li X 2016 A pedestrian flow model considering the impact of local density: voronoi diagram based heuristics approach *Transp. Res. C* **68** 566–80
- [21] Jin C J, Wang W, Jiang R and Dong L Y 2016 Simulating pedestrian flow by an improved two-process cellular automaton model *Int. J. Mod. Phys. C* **1750016**
- [22] Bandini S, Mondini M and Vizzari G 2014 Modelling negative interactions among pedestrians in high density situations *Transp. Res. C* **40** 251–70
- [23] Feliciani C and Nishinari K 2016 An improved cellular automata model to simulate the behavior of high density crowd and validation by experimental data *Physica A* **451** 135–48
- [24] Blue V J and Adler J L 1998 Emergent fundamental pedestrian flows from cellular automata microsimulation *Transp. Res. Rec.* **1644** 29–36
- [25] Blue V J and Adler J L 1978 Cellular automata microsimulation of bi-directional pedestrian flows *Transp. Res. Rec.* **1678** 135–41
- [26] Blue V J and Adler J L 2001 Cellular automata micro-simulation for modeling bi-directional pedestrian walkways *Transp. Res. B* **35** 293–312
- [27] Chattaraj U, Seyfried A and Chakroborty P 2009 Comparison of pedestrian fundamental diagram across cultures *Adv. Complex Syst.* **12** 393
- [28] Barlovic R, Santen L, Schadschneider A and Schreckenberg M 1998 Metastable states in cellular automata for traffic flow *Eur. Phys. J. B* **5** 793–800